



Multi–Proxy Reconstructions of Climate Change and Human Impacts Over the Past 7000 Years From an Archive of Continental Shelf Sediments off Eastern Hainan Island, China

Chao Huang^{1,2}, Deming Kong¹, Fajin Chen^{1*}, Jianfang Hu³, Peng Wang¹ and Junchuan Lin¹

¹Key Laboratory of Climate, Resources and Environment in Continental Shelf Sea and Deep Sea of Department of Education of Guangdong Province, Guangdong Ocean University, Zhanjiang, China, ²State Key Laboratory of Loess and Quaternary Geology, Institute of Earth Environment, Chinese Academy of Sciences, Xi'an, China, ³State Key Laboratory of Organic Geochemistry, Guangzhou Institute of Geochemistry, Chinese Academy of Sciences, Guangzhou, China

OPEN ACCESS

Edited by:

Min-Te Chen,
National Taiwan Ocean University,
Taiwan

Reviewed by:

Yu Li,
Lanzhou University, China
Asif Ali,
Anna University, Chennai, India

*Correspondence:

Fajin Chen
fjchen@gdou.edu.cn

Specialty section:

This article was submitted to
Quaternary Science, Geomorphology
and Paleoenvironment,
a section of the journal
Frontiers in Earth Science

Received: 03 February 2021

Accepted: 31 May 2021

Published: 14 June 2021

Citation:

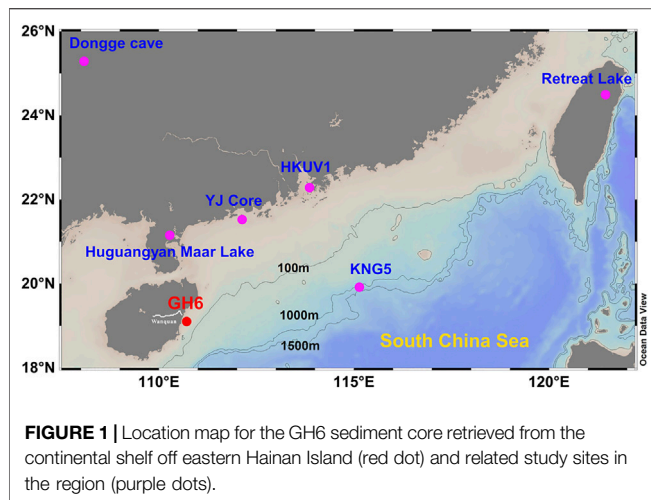
Huang C, Kong D, Chen F, Hu J,
Wang P and Lin J (2021) Multi–Proxy
Reconstructions of Climate Change
and Human Impacts Over the Past
7000 Years From an Archive of
Continental Shelf Sediments off
Eastern Hainan Island, China.
Front. Earth Sci. 9:663634.
doi: 10.3389/feart.2021.663634

Abrupt climatic events and the history of human activities on Hainan Island are poorly understood, due to the lack of high-resolution records. We present high-resolution multiproxy records from the coastal shelf off eastern Hainan Island in China to investigate abrupt climate change and regional human–environment interaction over the last 7,000 years. A prominent climatic anomaly occurred during 5,400–4,900 cal yr BP. This abrupt monsoon failure has been detected in various paleoclimatic records from monsoonal regions. Anomalous summer monsoon intensity during 5,400–4,900 cal yr BP is probably driven by solar variability, ENSO activity and ice-rafting events in the North Atlantic. Over the past 1,500 years, with the growing population and progress in production technology, human activity has increasingly become the dominant factor controlling the natural environment of Hainan Island.

Keywords: Asian summer monsoon, holocene, human activity, abrupt climate change, chemical weathering, terrigenous influx

INTRODUCTION

Extreme weather events are becoming more frequent owing to global warming, and people are increasingly concerned about climate change and its impacts on their lives. Over recent Earth history, several abrupt global climatic anomalies occurred during the Holocene (Bond et al., 2001; Mayewski et al., 2004; Wanner et al., 2011). For example, the 4200 BP climate event and the Little Ice Age, these events had disastrous consequences for humans, and seriously influenced the development of agriculture and the prehistoric advancement of human society (Cullen et al., 2000; DeMenocal, 2001; Douglas et al., 2016; Sinha et al., 2019). Climatic anomaly around 5,500 cal yr BP have recently received attention as a result of the close linkage between climate change and the evolution of prehistoric culture (Shuman, 2012; Bai et al., 2017; Wu et al., 2018; Hou and Wu, 2021; Tan et al., 2020). A detailed understanding of abrupt climatic events in the past is therefore critical for exploring their underlying forcing mechanisms and dealing with abrupt changes in the climate system in the future.



In recent years, studies have suggested that human activities play an important role in controlling ecosystems and soil erosion in monsoonal China. Increases in χ_{If} and χ_{fd} over the last 2000 years in sediments from the Yangtze delta in eastern China, Lake Xiaolongwan in northeast China, and lakes Erhai and Xingyun in southwest China reflect an increase in soil erosion attributed to enhanced human activity (Dearing et al., 2008; Wang et al., 2010; Su et al., 2015; Wu et al., 2015). Numerous studies likewise found that increasing contents of various metals, including Cu, Pb, and Zn, could be closely linked to mining and metalworking activities, reflecting a progressive intensification of human activities (Zong et al., 2010; Hu et al., 2013; Hillman et al., 2014; Wan et al., 2015; Xu et al., 2017; Huang et al., 2018). Additionally, pollen and black carbon results indicate significantly accelerated deforestation in monsoonal China since 2000 cal yr BP (Zhao et al., 2010; Ma et al., 2016a; Cheng et al., 2018; Lu et al., 2019; Pei et al., 2020).

As human populations grew and progress in production technology increased, human influences on the natural environment became increasingly important during the late Holocene, and often obscure the detection of climatic fluctuations in the archives investigated. Human activities can mediate the terrestrial ecosystems and soil erosion, generating unavailability of the relevant proxy indicators to reconstruct climate change. It is therefore essential to understand climate and human activities, as well as their impacts upon terrestrial ecosystems on longer timescales, in order to reconstruct each of them accurately. However, previous studies to determine human—environment interactions were mainly dependent on sediment cores from lakes (Dearing et al., 2008; Hillman et al., 2014; Su et al., 2015) and river deltas (Wang et al., 2010; Zong et al., 2010; Strong et al., 2013). High-resolution records from continental shelves are relatively scarce. Well dated and high-resolution data of various geologic archives from wide regions are crucial for better understanding the complex interplays between humans and the Earth. Sediment cores from continental shelves would therefore provide an excellent opportunity to understand human—environment interactions at regional scales.

Hainan Island, the second largest island in the northern South China Sea (SCS), is sensitive to climatic fluctuations. Previous studies have confirmed that continental shelf sediments off eastern Hainan provide valuable information on paleoclimate variation and human activity (Liu et al., 2013; Wu et al., 2017; Xu et al., 2017; Ji et al., 2020). However, most previous studies have focused on short timescales during the past 200 years (Liu et al., 2013; Wu et al., 2017). Accurate timing and intensity of human activity have not been well constrained. This study presents a high-resolution multi-proxy record with a robust chronology spanning the last 7,000 years collected from the continental shelf off eastern Hainan. The main aims are to investigate the interaction between Holocene climate variability, human activity and environmental changes, and to determine the timing and intensity of human activity on Hainan Island during the last 1,500 years.

MATERIALS AND METHODS

Materials

Hainan Island is the second largest island in the northern SCS and has an area of $\sim 33.9 \times 10^3 \text{ km}^2$ (Figure 1). The Wanquan River is the third largest river on the island and originates from the Wuzhishan Mountains. It drains southeast Hainan and eventually discharges into the northwestern SCS at Boao Township in Qionghai City. The river's total length is $\sim 157 \text{ km}$ and its drainage area covers $3,693 \text{ km}^2$ (Yang et al., 2013). The study region is dominated by a tropical monsoon climate (Zeng and Zeng, 1989). The annual mean temperature is $22.8\text{--}25.8^\circ\text{C}$. Annual precipitation ranges $961\text{--}2,439 \text{ mm yr}^{-1}$, with about 80% occurring during the wet season from April to September (Zhang et al., 2013).

The GH6 core ($19^\circ 06' \text{N}$, $110^\circ 42.85' \text{E}$; 2.4 m in length) was collected using a gravity corer from approximately 50 m water

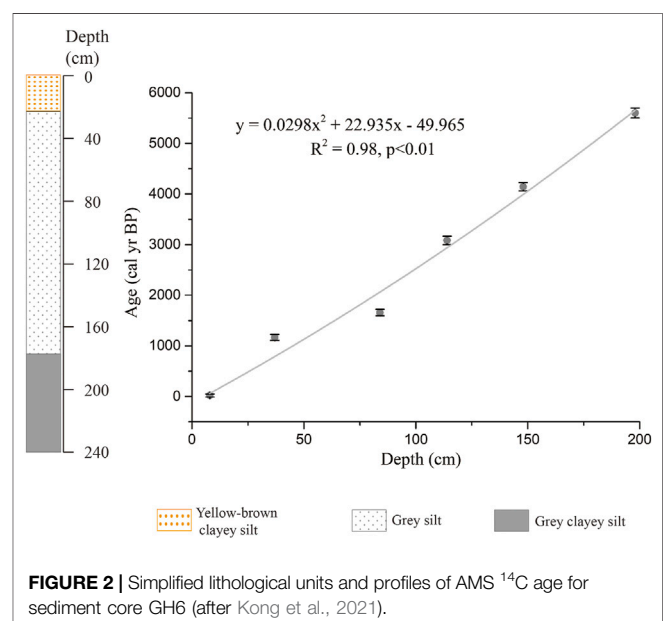


TABLE 1 | Details of 6 AMS ^{14}C dates from the GH6 core (after Kong et al., 2021).

Sample Code	Beta Lab Code	Depth (cm)	Material	Conventional age (years, BP)	Error (2 σ)	Calibrated	Error (2 σ)
						Age (years, BP)	
GH6-F10	530613	8	Foraminifera	460	30	20	30
GH6-F17	530614	37	Foraminifera	1,760	30	1,165.5	60
GH6-F84	530615	84	Foraminifera	2,240	30	1,656.5	65
GH6-F114	545408	114	Foraminifera	2,980	30	3,085	84.5
GH6-F148	532199	148	Foraminifera	4,230	30	4,142	81.5
GH6-F198	532200	198	Foraminifera	5,420	30	5,599.5	96.5

depth on the continental shelf off eastern Hainan Island (Figure 1). The sediment core was cut longitudinally and samples were stored at 4°C prior to analysis. As shown in Figure 2, GH6 core can be divided into three lithological units: Unit 1 (0–20 cm) consists of yellow-brown clayey silt; Unit 2 (20–176 cm) consists of grey silt containing occasional shells; and Unit 3 (176–240 cm) consists of grey clayey silt.

Age Model

The chronology for the GH6 core was based on six AMS ^{14}C dates from mixed species of planktonic foraminifera (Table 1; Figure 2). 10 mg of complete and clean planktonic foraminifera were selected hand-picked under a binocular dissecting microscope at 40 \times magnification and cleaned by sonication in deionized water in order to remove surface adhesions. AMS ^{14}C dates were measured at the BETA Laboratory in the United States. All radiocarbon dates were calibrated to calendar ages with Calib 8.1.0 software using the marine20 program (Reimer et al., 2020). The age models of each sample are established by Polynomial ($n = 2$) fitting between these calibrated ages. The average temporal resolution is ~ 58 years, and the average sedimentation rate is 0.03 cm/yr. For further details of the dating method and modelling approach, see Kong et al. (2021).

Major and Trace Element Compositions

Bulk sediment samples were freeze-dried and ground, then heated at 650°C for 4 h to remove organic matter. The samples were digested in an $\text{HNO}_3 + \text{HF}$ acid mixture and the solutions then used for major and trace-element analyses at 2-cm intervals. Major element concentrations were measured on a Varian 720 ES inductively coupled plasma—atomic emission spectrometer (ICP—AES). Trace element concentrations were measured on a Varian 820 inductively coupled plasma—mass spectrometer (ICP—MS). Precision and accuracy were monitored by analysing several United States Geological Survey (USGS) and Chinese certified reference standards (BHVO-2, BCR-2, GBW07314, GBW07315, GBW07316), yielding values that were generally within $\pm 10\%$ (RSD) of the certified values.

The chemical index of alteration (CIA), defined as $\text{Al}_2\text{O}_3 / (\text{Al}_2\text{O}_3 + \text{CaO} + \text{Na}_2\text{O} + \text{K}_2\text{O}) \times 100$, using molecular proportions, has been widely used as an indicator of chemical weathering intensity (Nesbitt and Young, 1982). In this study, it was difficult to evaluate the CaO content of the silicate fraction. The CIA was therefore calculated using the following formula,

excluding CaO: molar $\text{Al}_2\text{O}_3 / (\text{Al}_2\text{O}_3 + \text{Na}_2\text{O} + \text{K}_2\text{O}) \times 100$ (Arnaud et al., 2012; Liu et al., 2014). This amendment does not have a significant effect on the results because only relative variations in chemical weathering are considered (Arnaud et al., 2012).

Environmental Magnetic Measurements

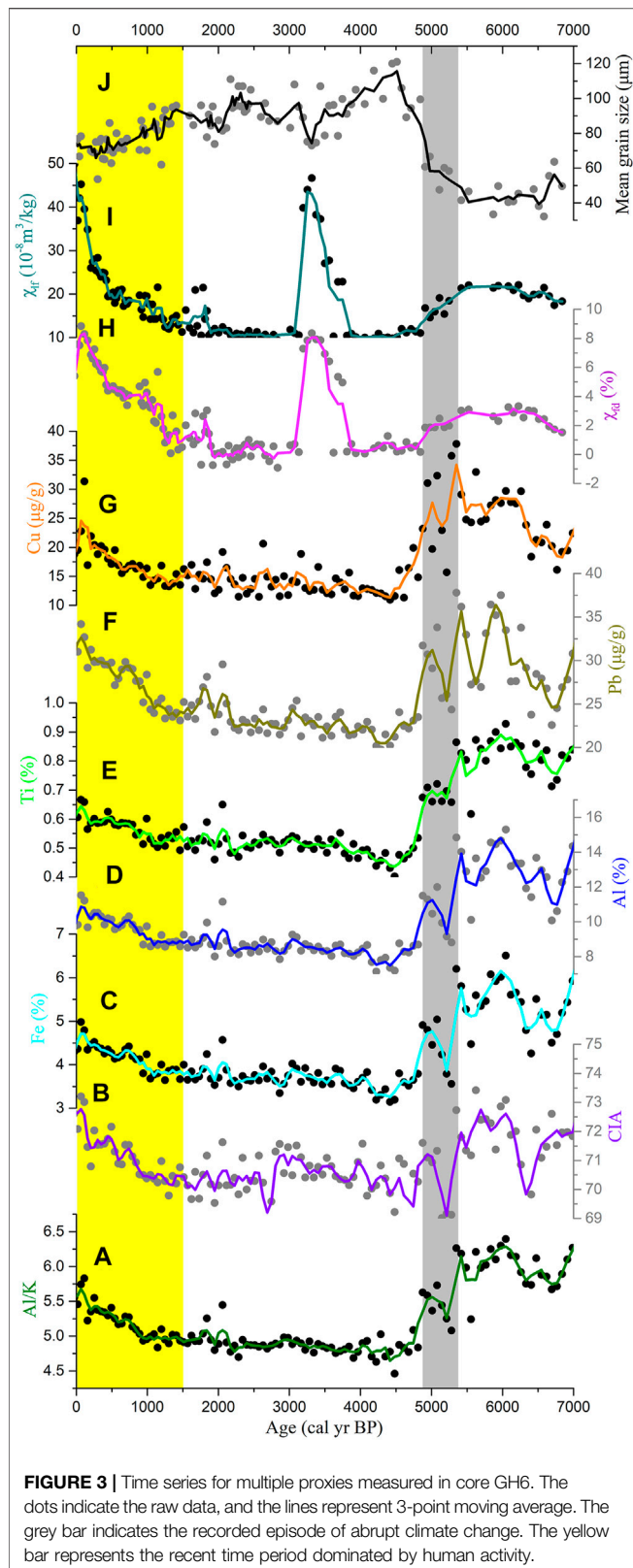
Magnetic susceptibility was determined at about 1–6 cm intervals. The low-field magnetic susceptibility (χ) for all discrete samples was measured using a Kappabridge MFK1-FA (AGICO) magnetic susceptibility meter at low (976 Hz) and high (15,616 Hz) frequencies (defined as χ_{lf} and χ_{hf} respectively). Frequency-dependent magnetic susceptibility ($\chi_{\text{fd}}\%$) was calculated using the formula $\chi_{\text{fd}}\% = 100 \times (\chi_{\text{lf}} - \chi_{\text{hf}}) / \chi_{\text{lf}}$.

Particle Size Analysis

The samples used for the particle-size analysis were collected at about 1–7 cm intervals. All samples were pre-treated with 10% H_2O_2 , followed by treatment with 10% HCl, to remove organic matter and carbonates, respectively. They were then rinsed with deionized water and dispersed with 10 ml of 0.05 mol L^{-1} $(\text{NaPO}_3)_6$ on an ultrasonic vibrator for 10 min. The grain-size distribution was measured using a Malvern 3,000 laser diffraction instrument. Mean grain size was calculated according to Folk and Ward (1957).

RESULTS

As shown in Figure 3, the Al/K, CIA, Al, Fe, Ti, Cu and Pb values share very similar trends through time. Generally, the variations in multi-proxies of GH6 core can be divided into four stages. During the interval 7,000–5,400 cal yr BP, CIA values and Al/K ratios are relatively high, and contents of Al, Fe, Ti, Cu, and Pb are also relatively high; both χ_{lf} and χ_{fd} values remain relatively high, but the mean grain size has relatively low values. During the interval 5,400–4,900 cal yr BP, all of proxies in GH6 core show an abrupt shift; a sharp decrease in CIA and Al/K ratios is observed, and contents of Al, Fe, Ti, Cu, and Pb exhibit clear decreasing trends; both χ_{lf} and χ_{fd} values show a rapid decrease, but the mean grain size exhibits a rapid increase. During the interval 4,900–1,500 cal yr BP, CIA and Al/K ratios are relatively low, and contents of Al, Fe, Ti, Cu, and Pb remain fairly constant and relatively low values; both χ_{lf} and χ_{fd} values are relatively low except the period of 4,000–3,200 cal yr BP, and prominent peaks



of them would be attributed the pedogenic process; the mean grain size show a rapid increase. After 1,500 cal yr BP, CIA, and Al/K exhibit clear increasing trends, and contents of Al, Fe, Ti,

Cu, and Pb show an overall increasing trend; both χ_{fr} and χ_{cl} values show an overall increase, and the mean grain size exhibits an overall decreasing trend.

DISCUSSION

Palaeoclimatic Significance of Proxy Indicators

Different elements behave differently during chemical weathering processes. Elemental ratios can therefore be applied to indicate variations in chemical weathering intensity. K tends to be enriched in weathering products after moderate chemical weathering (Nesbitt et al., 1980; Condie et al., 1995), whereas Al tends to be retained and enriched in weathering products (Nesbitt and Markovics, 1997; Nesbitt et al., 1980). Thus, Al/K ratios can be used to reflect the intensity of chemical weathering, with higher Al/K ratios indicating stronger chemical weathering. In our core GH6, Al/K ratios exhibit similar variations to CIA values (Figures 3A,B). The latter have been widely used to trace the intensity of chemical weathering; e.g., core KNG5 from the northern SCS slope (Huang et al., 2015), core YJ from the northern SCS inner shelf (Huang et al., 2018), and core 337 PC from the Qiongdongnan Basin (Wan et al., 2015). In addition, Al/K ratios have been successfully used to indicate variations in chemical weathering intensity in the northern SCS and the Pearl River delta (Wei et al., 2006; Hu et al., 2012; Hu et al., 2013; Clift et al., 2014). This provides further evidence that Al/K ratios can be employed as an indicator of chemical weathering intensity.

Climate is believed to be the dominant factor controlling the degree of chemical weathering under specific environmental conditions (White and Blum, 1995). Warm and humid conditions favour intense chemical weathering, with humidity playing the more important role (White and Blum, 1995; West et al., 2005; Gabet et al., 2006). Previous studies have confirmed that sediments on the continental shelf off Hainan in the northern SCS were primarily derived from the island itself (Tian et al., 2013; Hu et al., 2014; Yan et al., 2016; Xu et al., 2017). Hainan currently experiences a humid tropical climate that is strongly influenced by the Asian summer monsoon (Liu et al., 1999). The proxies for chemical weathering (CIA and Al/K) in core GH6 can therefore be used to trace the strength of the summer monsoon.

In marine sediments, concentrations of Al, Ti, and Fe are primarily derived from terrigenous detrital materials (Latimer and Filippelli, 2001; Ishfaq et al., 2013). Thus, these elements are widely employed as a tracer of terrigenous influx in marine sediments (Haug et al., 2001; Peterson and Haug, 2006; Revel et al., 2010). Al, Ti, and Fe variations in core YJ from the northern inner shelf of the SCS have been successfully used to indicate changes in terrigenous influx (Huang et al., 2019). This provides further evidence that Al, Ti, and Fe concentrations in our GH6 core can be used to trace changes in terrigenous sediment input. In southern China, numerous studies have confirmed that continental erosion is primarily associated with monsoon precipitation, with heavier monsoon precipitation causing

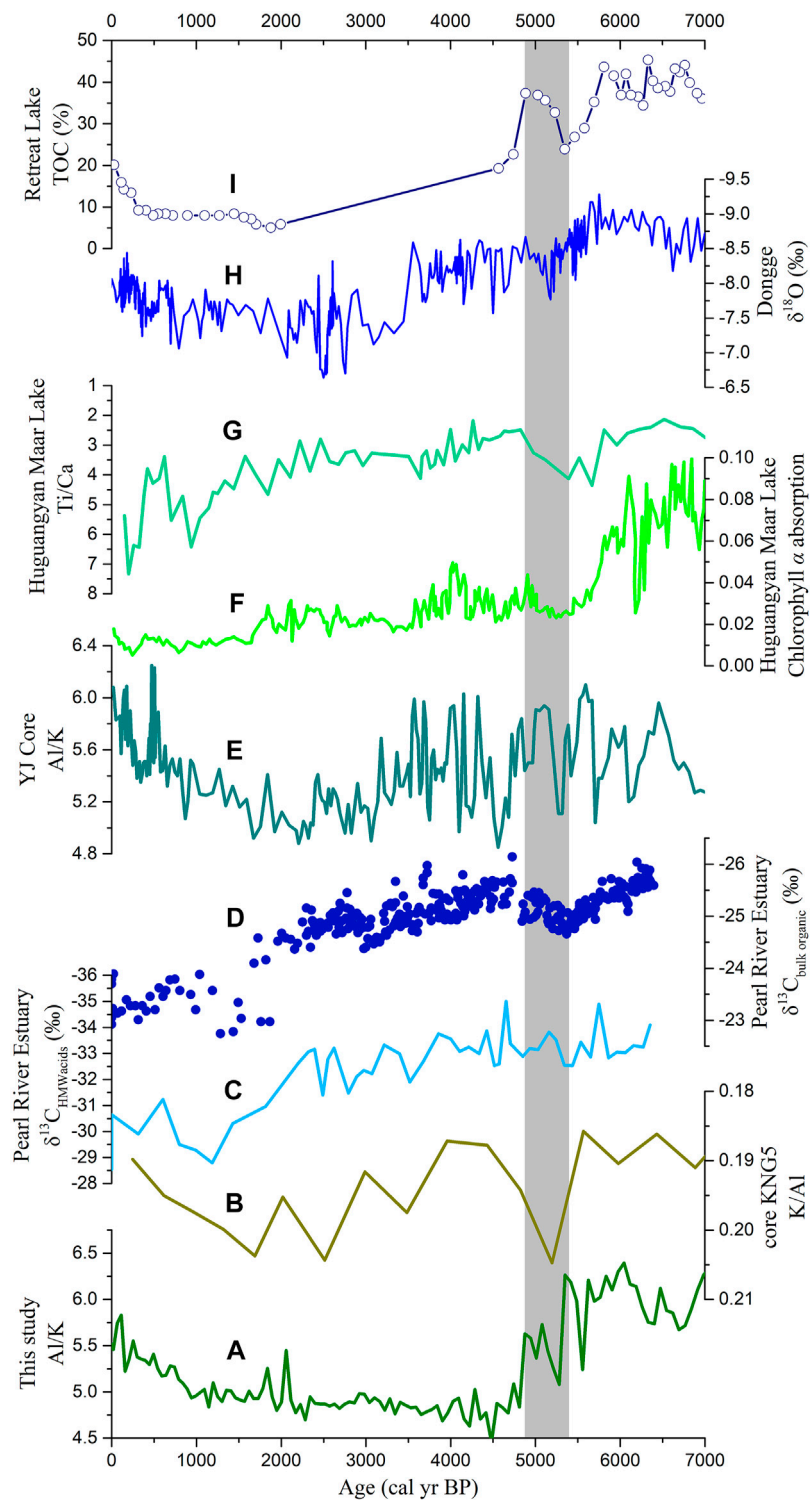


FIGURE 4 | Comparisons between related records: **(A)** Al/K ratios from our GH6 core; **(B)** K/Al record from the northern South China Sea slope (Huang et al., 2016); **(C)** compound-specific $\delta^{13}\text{C}$ record from the Pearl River Estuary (Strong et al., 2013); **(D)** $\delta^{13}\text{C}_{\text{org}}$ record from the Pearl River Estuary (Yu et al., 2012); **(E)** Al/K ratios from the northern inner shelf of the South China Sea (Huang et al., 2019); **(F)** chlorophyll- α record from Huguangyan Maar Lake (Wu et al., 2012); **(G)** Ti/Ca record from Huguangyan Maar Lake (Shen et al., 2013); **(H)** stalagmite $\delta^{18}\text{O}$ record from Dongge Cave (Dykoski et al., 2005); and **(I)** TOC data from Retreat Lake in northeastern Taiwan (Selvaraj et al., 2007).

greater terrigenous influx (Hu et al., 2012; Clift et al., 2014; Wan et al., 2015; Huang et al., 2019). Furthermore, Al, Ti, and Fe variations in our GH6 core, as proxies for terrigenous influx, show similar temporal patterns to CIA and Al/K ratios throughout the core. Consequently, we can reasonably speculate that stronger monsoon precipitation generates greater chemical weathering and associated volumes of terrigenous inputs.

Abrupt Changes in Summer Monsoon Strength 5,400–4,900 cal yr BP and Forcing Mechanisms

During the period 5,400–4,900 cal yr BP, the intensity of chemical weathering decreased rapidly, as inferred from the profiles of CIA and Al/K in our GH6 core. The terrigenous influx decreased rapidly during the same interval, as indicated by concentrations of Al, Ti, and Fe. Simultaneously, the mean sediment grain size increased sharply. The distinct variations in these records suggest a rapid climatic deterioration, which was likely associated with abrupt changes in the Asian summer monsoon. This abrupt climatic event generally coincides with a dramatic weakening of the summer monsoon at 5,400–4,900 cal yr BP, as inferred from various paleoclimate records from monsoonal regions elsewhere (Dykoski et al., 2005; Strong et al., 2013; Huang et al., 2019; Shah et al., 2020).

Chemical weathering interpreted from core KNG5, retrieved from the northern SCS slope, shows an abrupt decrease, reflecting reduced monsoon rainfall (Figure 4B; Huang et al., 2016). In the Pearl River estuary, abrupt summer monsoon failure can be detected in bulk-sedimentary $\delta^{13}\text{C}_{\text{org}}$ and compound-specific $\delta^{13}\text{C}$ records (Figures 4C,D; Yu et al., 2012; Strong et al., 2013). In the northern inner shelf of the SCS, Al/K ratios, used as an indicator of chemical weathering, exhibit a rapid decrease in response to the weakening monsoon (Figure 4E; Huang et al., 2019). This sudden climate shift is also documented in terrestrial sediment records in southern China. In Huguangyan Maar Lake, the weak summer monsoon during this period is detected from multiple climatic indices, including records of chlorophyll α and TOC (Figure 4F; Wu et al., 2012), Ti/Ca ratios (Figure 4G; Shen et al., 2013), and magnetic properties (Duan et al., 2014). Similarly, a positive shift in the stalagmite $\delta^{18}\text{O}$ record from Dongge Cave implies a weakening of the summer monsoon (Figure 4H; Dykoski et al., 2005). The development of stagnant swampy environments in the northern Wuyi Mountains is also attributed to a decline in the summer monsoon (Ma et al., 2016b). Within age uncertainty, the subalpine Retreat Lake in Taiwan also experienced an abrupt weak monsoon event, as indicated by low TOC (Figure 4I; Selvaraj et al., 2007). Taken together, these multiple proxy records from various geological archives in southern China capture this abrupt climatic shift (Figure 4). In addition, the event can similarly be detected across different monsoonal regions of China (An et al., 2012; Li et al., 2017a; Bai et al., 2017; Goldsmith et al., 2017; Tan et al., 2020).

As shown in Figure 5, the weak monsoon between 5,400 and 4,900 cal yr BP, recorded in our GH6 core, shows good correspondence within dating uncertainty with an interval of weak solar activity as inferred from residual atmospheric ^{14}C

($\Delta^{14}\text{C}$) (Stuiver, et al., 1998) and ice core ^{10}Be data (Steinhilber et al., 2009). This synchronicity suggests a causal linkage between solar activity and summer monsoon variability. In fact, previous studies have linked weak monsoon events to solar activity (Huang et al., 2019). The solar–monsoon link can be explained by a direct influence: solar forcing may control monsoon precipitation by regulating the land–sea thermal contrast (Liu et al., 2009; Xu et al., 2015). A decline in solar output would decrease the land–sea thermal contrast, subsequently leading to southward movement of the Intertropical Convergence Zone (ITCZ). Reduced transportation of water vapour from the ocean to the continents thereby causes less rainfall over monsoonal Asia (Fleitmann et al., 2003; Dykoski et al., 2005; Li et al., 2017b).

In addition, solar activity may influence variability in the summer monsoon indirectly, perhaps amplified by North Atlantic teleconnection and El Niño–Southern Oscillation (ENSO) activity (Wang et al., 2005; 2016; Marchitto et al., 2010). During the period 5,400–4,900 cal yr BP, the weaker monsoon inferred from our GH6 core coincides with higher percentages of hematite-stained grains in the North Atlantic, which can be taken as an indication of ice-rafted debris (IRD) (Figure 5D; Bond et al., 2001). Reduced solar activity may trigger IRD events in the North Atlantic (Bond et al., 2001) and a slowdown of North Atlantic meridional overturning circulation (AMOC) (Oppo et al., 2003), eventually weakening the summer monsoon. Likewise, the abrupt summer monsoon failure during this period is also consistent with strong ENSO activity, indicated by sea surface temperature (SST) records from the Western Pacific Warm Pool (Figure 5E; Stott et al., 2004). Previous studies have confirmed that ENSO may act as a mediator between solar energy input and the Asian summer monsoon (Asmerom et al., 2007; Emile-Geay et al., 2007; Marchitto et al., 2010). These results suggest a link between East Asia, the tropical Pacific and the North Atlantic: a potential forcing mechanism for abrupt climate change is that solar variability can affect the Asian summer monsoon via the North Atlantic and the ENSO system.

Human Disturbance Over the Past 1,500 Years

As shown in Figure 6, some decoupling have been observed between records of climate, chemical weathering and fluvial discharge over the past 1,500 years. Temperature reconstructions for the Northern hemisphere and the whole of China exhibit an overall cooling trend (Figures 6A,B; Yang et al., 2002; PAGES 2k Consortium, 2013). There is a general decrease in the intensity of monsoonal precipitation during this period, as inferred from pollen-reconstructed annual rainfalls from Gonghai Lake and annual mean precipitation reconstructions in northern China (Figures 6C,D; Chen et al., 2015; Li et al., 2017b). Similarly, a long-term decrease in monsoon precipitation can be found in high-resolution stalagmite $\delta^{18}\text{O}$ records from Dongge and Heshang caves in southern China (Wang et al., 2005; Hu et al., 2008).

However, values of CIA and Al/K ratios in our GH6 core show an overall increasing trend during the last 1,500 years

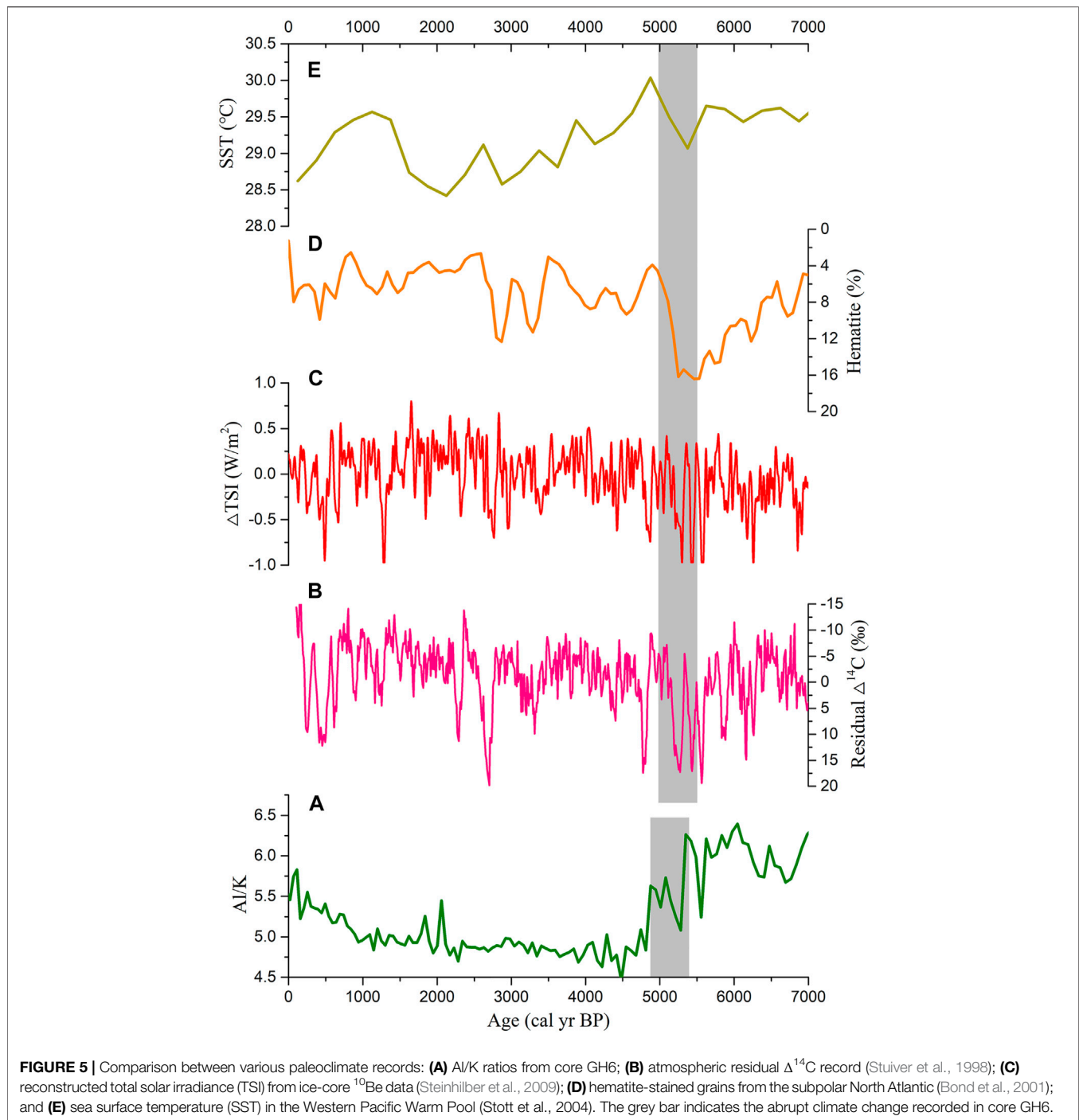


(Figure 6E), reflecting enhanced chemical weathering. An overall increasing trend of terrigenous supply can be also seen, as indicated by concentrations of Al, Ti, and Fe (Figure 6F). These trends suggest that climate alone cannot be responsible for changes in chemical weathering and fluvial influx. The concentrations of Cu and Pb in the GH6 core increase dramatically over the past 1,500 years (Figures 6G,H). Previous studies have confirmed that increasing metal contents (Cu, Pb, and Zn) appear to be associated with mining and

smelting activities (Hu et al., 2013; Hillman et al., 2014; Wan et al., 2015; Huang et al., 2018). Moreover, χ_{If} and χ_{fd} values in core GH6 exhibit a striking increase over the same period. Mounting evidence suggests that such increases in χ_{If} and χ_{fd} can be attributed to human-induced soil erosion (Dearing et al., 2008; Wang et al., 2010; Wu et al., 2015; Huang et al., 2018).

More importantly, all of the proxies in our GH6 core are generally consistent with the historical exploitation of Hainan Island (Figure 7; Situ, 1987). This provides further evidence for

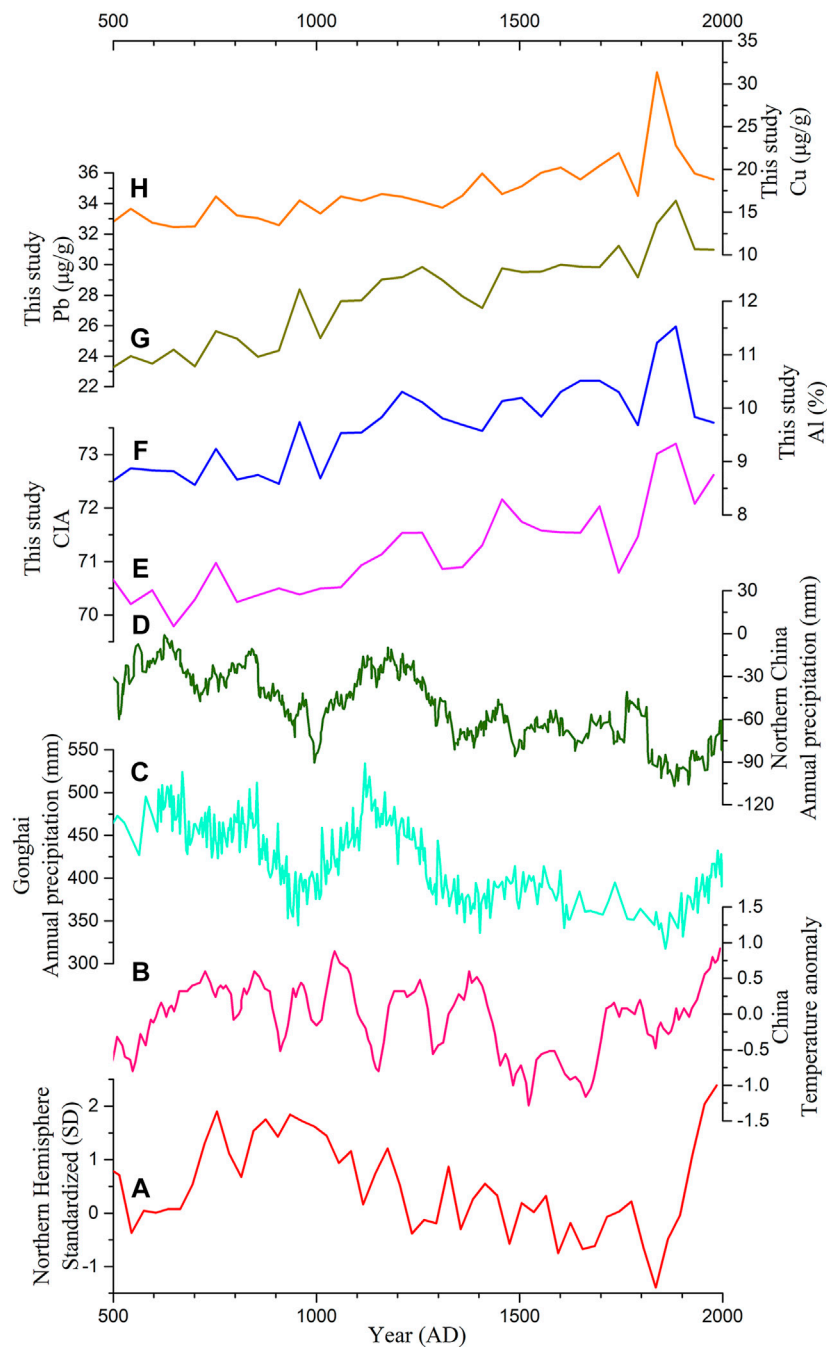
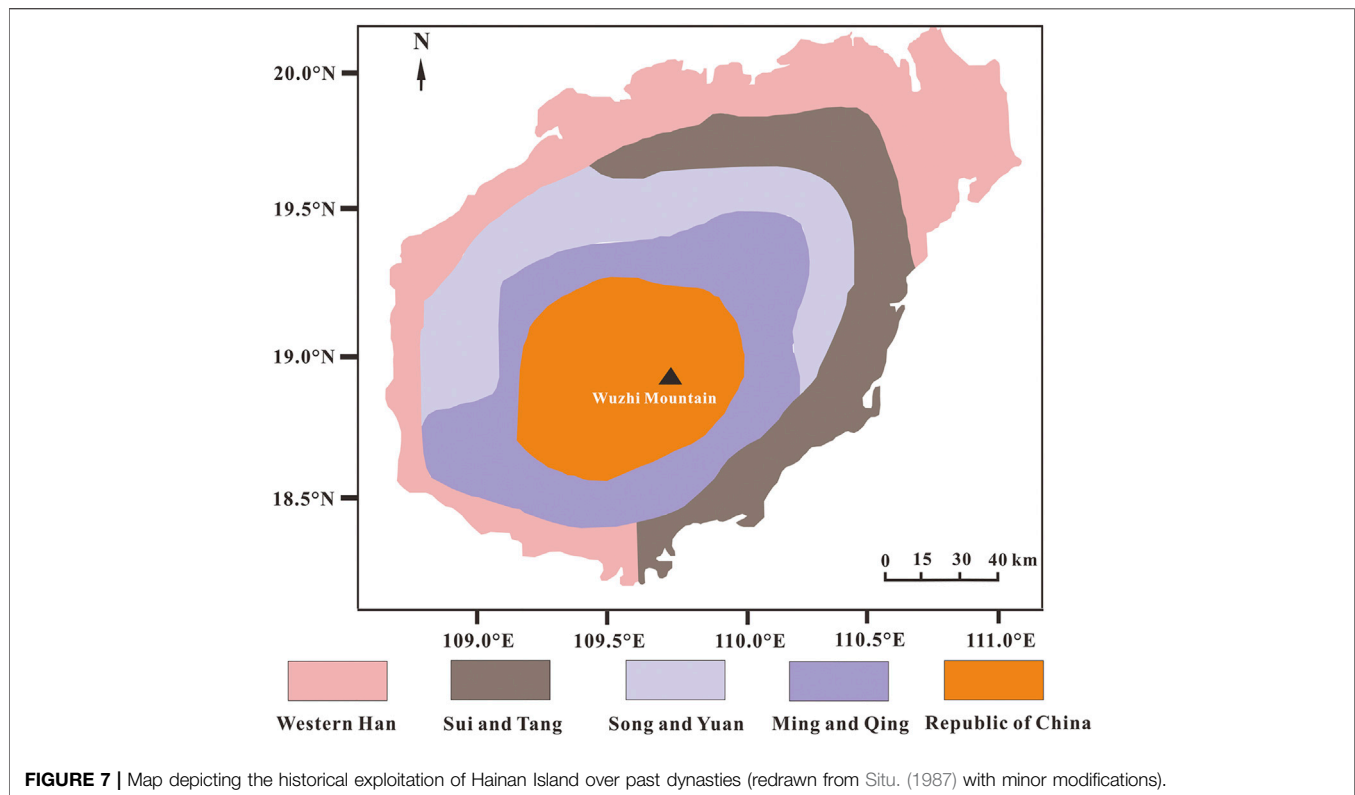


FIGURE 6 | Comparison between GH6 core records and temperature and precipitation data: **(A)** standardized 30-years-mean temperature record averaged over the whole Northern Hemisphere (PAGES 2k Consortium, 2013); **(B)** temperature reconstructions for the whole of China (Yang et al., 2002); **(C)** pollen-inferred annual precipitation data from Gonghai Lake (Chen et al., 2015); **(D)** KCM-based annual precipitation record for northern China (Li et al., 2017b); **(E–H)** multiple proxies from GH6 core.

increasing influence of human activities over the last 1,500 years. According to historical documents, the first large-scale immigration from mainland China took place during the Sui and Tang Dynasty (581–907 AD), with the majority of migrants settling in eastern coastal areas of Hainan (Figure 7; Situ, 1987). Migrant numbers increase dramatically during the Song Dynasty.

These migrants brought advanced tools and cultivation techniques, such as metalworking and Champa rice (Situ, 1987). The advent of metal tools and metalworking activities may be responsible for the increasing concentrations of Cu and Pb in core GH6 during the past 1,500 years. Population expansion and advanced cultivation techniques would have accelerated



deforestation for farming and caused reworking of older highly-weathered materials. This probably enhanced the input of terrestrial material, sourced more deeply and from a wider area. These effects correspond to the increase of proxy indicators in our GH6 core (i.e., CIA, Al/K, χ_{lf} , χ_{fd} , Al, Ti, Fe, Cu, and Pb). Consequently, we can reasonably conclude that human activities have had a growing influence on the natural environment and landscape in eastern Hainan over the past 1,500 years.

CONCLUSION

This study presents high-resolution multi-proxy analyses incorporating chronological, environmental-magnetic, geochemical and grain-size evidence from the coastal shelf off eastern Hainan Island, China. The prominent climatic anomaly during 5,400–4,900 cal yr BP is observed, which coincides with a dramatic weakening of the summer monsoon. This abrupt event is synchronous with a period of weak solar activity, strong El Niño-Southern Oscillation (ENSO) activity and North Atlantic ice-rafting. These results suggest a climatic link between East Asia, the tropical Pacific and the North Atlantic. The possible forcing mechanism for abrupt climate change is solar variability affecting the Asian summer monsoon via the North Atlantic and ENSO system. There are some decoupling between records of climate, chemical weathering and fluvial discharge over the past 1,500 years. Moreover, enhanced chemical weathering and terrigenous influx during the past 1,500 years are consistent

with increasing metal contents (Cu and Pb), and increases in magnetic susceptibility (χ_{lf}) and frequency-dependent magnetic susceptibility (χ_{fd}). All of these proxies are generally consistent with the historical exploitation of Hainan Island. We therefore suggest that enhanced human activity (deforestation, cultivation and mining) over the past 1,500 years has overwhelmed the natural climatic controls on the environment and landscape of Hainan Island.

DATA AVAILABILITY STATEMENT

The original contributions presented in the study are included in the article/**Supplementary Material**, further inquiries can be directed to the corresponding author.

AUTHOR CONTRIBUTIONS

FC and CH designed the study; CH, DK, JH, PW, and JL performed research; CH analyzed data and contributed to data interpretation and paper writing. All authors contributed to the discussion and interpretation of the results and to the writing of the manuscript.

FUNDING

This work was financially supported by National Natural Science Foundation of China (Nos. 42001078, U1901213, 41876058,

41991252), Guangdong Natural Science Foundation of China (No. 2020A1515010500), Open Fund of the State Key Laboratory of Loess and Quaternary Geology, Institute of Earth Environment, CAS (SKLLQG 1908), and Marine Science Research Team Project of Guangdong Ocean University (No. 002026002004).

REFERENCES

- An, Z., Colman, S. M., Zhou, W., Li, X., Brown, E. T., Jull, A. J. T., et al. (2012). Interplay between the Westerlies and Asian Monsoon Recorded in lake Qinghai Sediments since 32 Ka. *Sci. Rep.* 2, 619. doi:10.1038/srep00619
- Arnaud, F., Révillon, S., Debret, M., Revel, M., Chapron, E., Jacob, J., et al. (2012). Lake Bourget Regional Erosion Patterns Reconstruction Reveals Holocene NW European Alps Soil Evolution and Paleohydrology. *Quat. Sci. Rev.* 51, 81–92. doi:10.1016/j.quascirev.2012.07.025
- Asmerom, Y., Polyak, V., Burns, S., and Rasmussen, J. (2007). Solar Forcing of Holocene Climate: New Insights from a Speleothem Record, Southwestern United States. *Geol.* 35, 1–4. doi:10.1130/g22865a.1
- Bai, Y., Zhang, P., Gao, T., Yu, R., Zhou, P., and Cheng, H. (2017). The 5400 a BP Extreme Weakening Event of the Asian Summer Monsoon and Cultural Evolution. *Sci. China Earth Sci.* 60, 1171–1182. doi:10.1007/s11430-016-9017-3
- Bond, G., Kromer, B., Beer, J., Muscheler, R., Evans, M. N., Showers, W., et al. (2001). Persistent Solar Influence on North Atlantic Climate during the Holocene. *Science* 294, 2130–2136. doi:10.1126/science.1065680
- Chen, F., Xu, Q., Chen, J., Birks, H. J., Liu, J., Zhang, S., et al. (2015). East Asian Summer Monsoon Precipitation Variability since the Last Deglaciation. *Sci. Rep.* 5, 11186. doi:10.1038/srep11186
- Cheng, Z., Weng, C., Steinke, S., and Mohtadi, M. (2018). Anthropogenic Modification of Vegetated Landscapes in Southern China from 6,000 Years Ago. *Nat. Geosci.* 11, 939–943. doi:10.1038/s41561-018-0250-1
- Clift, P. D., Wan, S., and Blusztajn, J. (2014). Reconstructing Chemical Weathering, Physical Erosion and Monsoon Intensity since 25Ma in the Northern South China Sea: A Review of Competing Proxies. *Earth-Science Rev.* 130, 86–102. doi:10.1016/j.earscirev.2014.01.002
- Condie, K. C., Dengate, J., and Cullers, R. L. (1995). Behavior of Rare Earth Elements in a Paleoweathering Profile on Granodiorite in the Front Range, Colorado, USA. *Geochimica et Cosmochimica Acta* 59, 279–294. doi:10.1016/0016-7037(94)00280-y
- Cullen, H. M., deMenocal, P. B., Hemming, S., Hemming, G., Brown, F. H., Guilderson, T., et al. (2000). Climate Change and the Collapse of the Akkadian empire: Evidence from the Deep Sea. *Geology* 28, 379–382. doi:10.1130/0091-7613(2000)028<0379:ccatco>2.3.co;2
- Dearing, J. A., Jones, R. T., Shen, J., Yang, X., Boyle, J. F., Foster, G. C., et al. (2008). Using Multiple Archives to Understand Past and Present Climate-Human-Environment Interactions: the lake Erhai Catchment, Yunnan Province, China. *J. Paleolimnol.* 40, 3–31. doi:10.1007/s10933-007-9182-2
- deMenocal, P. B. (2001). Cultural Responses to Climate Change during the Late Holocene. *Science (New York, N.Y.)* 292, 667–673. doi:10.1126/science.1059827
- Douglas, P. M. J., Demarest, A. A., Brenner, M., and Canuto, M. A. (2016). Impacts of Climate Change on the Collapse of lowland Maya Civilization. *Annu. Rev. Earth Planet. Sci.* 44, 613–645. doi:10.1146/annurev-earth-060115-012512
- Duan, Z., Liu, Q., Yang, X., Gao, X., Su, Y., and Su, Y. (2014). Magnetism of the Huguangyan Maar Lake Sediments, Southeast China and its Paleoenvironmental Implications. *Palaeogeogr. Palaeoclimatol. Palaeoecol.* 395, 158–167. doi:10.1016/j.palaeo.2013.12.033
- Dykoski, C., Edwards, R., Cheng, H., Yuan, D., Cai, Y., Zhang, M., et al. (2005). A High-Resolution, Absolute-Dated Holocene and Deglacial Asian Monsoon Record from Dongge Cave, China. *Earth Planet. Sci. Lett.* 233, 71–86. doi:10.1016/j.epsl.2005.01.036
- Emile-Geay, J., Cane, M., Seager, R., Kaplan, A., and Almasi, P. (2007). El Niño as a Mediator of the Solar Influence on Climate. *Paleoceanography* 22. doi:10.1029/2006pa001304

SUPPLEMENTARY MATERIAL

The Supplementary Material for this article can be found online at: <https://www.frontiersin.org/articles/10.3389/feart.2021.663634/full#supplementary-material>

- Fleitmann, D., Burns, S. J., Mudelsee, M., Neff, U., Kramers, J., Mangini, A., et al. (2003). Holocene Forcing of the Indian Monsoon Recorded in a Stalagmite from Southern Oman. *Science* 300, 1737–1739. doi:10.1126/science.1083130
- Folk, R. L., and Ward, W. C. (1957). Brazos River Bar [Texas]; a Study in the Significance of Grain Size Parameters. *J. Sediment. Res.* 27, 3–26. doi:10.1306/74d70646-2b21-11d7-8648000102c1865d
- Goldsmith, Y., Broecker, W. S., Xu, H., Polissar, P. J., deMenocal, P. B., Porat, N., et al. (2017). Northward Extent of East Asian Monsoon Covaries with Intensity on Orbital and Millennial Timescales. *Proc. Natl. Acad. Sci. USA.* 114, 1817–1821. doi:10.1073/pnas.1616708114
- Haug, G. H., Hughen, K. A., Sigman, D. M., Peterson, L. C., and Röhl, U. (2001). Southward Migration of the Intertropical Convergence Zone through the Holocene. *Science* 293, 1304–1308. doi:10.1126/science.1059725
- Hillman, A. L., Yu, J., Abbott, M. B., Cooke, C. A., Bain, D. J., and Steinman, B. A. (2014). Rapid Environmental Change during Dynastic Transitions in Yunnan Province, China. *Quat. Sci. Rev.* 98, 24–32. doi:10.1016/j.quascirev.2014.05.019
- Hou, M., and Wu, W. X. (2021). A Review of 6000–5000 Cal BP Climatic Anomalies in China. *Quat. Int.* 571, 58–72. doi:10.1016/j.quaint.2020.12.004
- Hu, B., Li, J., Cui, R., Wei, H., Zhao, J., Li, G., et al. (2014). Clay Mineralogy of the Riverine Sediments of Hainan Island, South China Sea: Implications for Weathering and Provenance. *J. Asian Earth Sci.* 96, 84–92. doi:10.1016/j.jseaes.2014.08.036
- Hu, C., Henderson, G. M., Huang, J., Xie, S., Sun, Y., and Johnson, K. R. (2008). Quantification of Holocene Asian Monsoon Rainfall from Spatially Separated Cave Records. *Earth Planet. Sci. Lett.* 266, 221–232. doi:10.1016/j.epsl.2007.10.015
- Hu, D., Böning, P., Köhler, C. M., Hillier, S., Pressling, N., Wan, S., et al. (2012). Deep Sea Records of the continental Weathering and Erosion Response to East Asian Monsoon Intensification since 14ka in the South China Sea. *Chem. Geology.* 326–327, 1–18. doi:10.1016/j.chemgeo.2012.07.024
- Hu, D., Clift, P. D., Böning, P., Hannigan, R., Hillier, S., Blusztajn, J., et al. (2013). Holocene Evolution in Weathering and Erosion Patterns in the Pearl River delta. *Geochem. Geophys. Geosyst.* 14, 2349–2368. doi:10.1002/ggge.20166
- Huang, C., Zeng, T., Ye, F., and Wei, G. (2019). Solar-forcing-induced Spatial Synchronisation of the East Asian Summer Monsoon on Centennial Timescales. *Palaeogeogr. Palaeoclimatol. Palaeoecol.* 514, 536–549. doi:10.1016/j.palaeo.2018.11.002
- Huang, C., Zeng, T., Ye, F., Xie, L., Wang, Z., Wei, G., et al. (2018). Natural and Anthropogenic Impacts on Environmental Changes over the Past 7500 Years Based on the Multi-Proxy Study of Shelf Sediments in the Northern South China Sea. *Quat. Sci. Rev.* 197, 35–48. doi:10.1016/j.quascirev.2018.08.005
- Huang, J., Wan, S., Xiong, Z., Zhao, D., Liu, X., Li, A., et al. (2016). Geochemical Records of Taiwan-Sourced Sediments in the South China Sea Linked to Holocene Climate Changes. *Palaeogeogr. Palaeoclimatol. Palaeoecol.* 441, 871–881. doi:10.1016/j.palaeo.2015.10.036
- Ishfaq, A. M., Pattan, J. N., Matta, V. M., and Banakar, V. K. (2013). Variation of Paleo-Productivity and Terrigenous Input in the Eastern Arabian Sea during the Past 100 Ka. *J. Geol. Soc. India* 81, 647–654. doi:10.1007/s12594-013-0086-7
- Ji, C., Xu, L., Zhang, Y., Guo, M., and Kong, D. (2020). A 1900-year Record of Mercury (Hg) from the East continental Shelf of Hainan Island, South China Sea. *Geol. J.* 55, 4469–4478. doi:10.1002/gj.3678
- Kong, D. M., Chen, G. S., Feng, W., J., Liu, Z. H., Chen, M. T., and Xu, L. Q. (2021). Alkenone-derived SST and Implication for Upwelling Changes off the Eastern Hainan Island over the Last 5000 Years. *Front. Earth Sci.* (submitted for publication).
- Latimer, J. C., and Filippelli, G. M. (2001). Terrigenous Input and Paleo-productivity in the Southern Ocean. *Paleoceanography* 16, 627–643. doi:10.1029/2000pa000586
- Li, J., Dodson, J., Yan, H., Cheng, B., Zhang, X., Xu, Q., et al. (2017a). Quantitative Precipitation Estimates for the Northeastern Qinghai-Tibetan Plateau over the

- Last 18,000 Years. *J. Geophys. Res. Atmos.* 122, 5132–5143. doi:10.1002/2016jd026333
- Li, J., Dodson, J., Yan, H., Zhang, D. D., Zhang, X., Xu, Q., et al. (2017b). Quantifying Climatic Variability in Monsoonal Northern China over the Last 2200 Years and its Role in Driving Chinese Dynastic Changes. *Quat. Sci. Rev.* 159, 35–46. doi:10.1016/j.quascirev.2017.01.009
- Liu, J., Chen, J., Selvaraj, K., Xu, Q., Wang, Z., and Chen, F. (2014). Chemical Weathering over the Last 1200 Years Recorded in the Sediments of Gonghai Lake, Lvlaiang Mountains, North China: a High-Resolution Proxy of Past Climate. *Boreas* 43, 914–923. doi:10.1111/bor.12072
- Liu, W. T., and Xie, X. (1999). Spacebased Observations of the Seasonal Changes of South Asian Monsoons and Oceanic responses. *Geophys. Res. Lett.* 26, 1473–1476. doi:10.1029/1999gl900289
- Liu, X., Dong, H., Yang, X., Herzsich, U., Zhang, E., Stuut, J., et al. (2009). Late Holocene Forcing of the Asian winter and Summer Monsoon as Evidenced by Proxy Records from the Northern Qinghai-Tibetan Plateau. *Earth Planet Sci. Lett.* 280, 276–284. doi:10.1016/j.epsl.2009.01.041
- Liu, Y., Peng, Z., Shen, C.-C., Zhou, R., Song, S., Shi, Z., et al. (2013). Recent 121-year Variability of Western Boundary Upwelling in the Northern South China Sea. *Geophys. Res. Lett.* 40, 3180–3183. doi:10.1002/grl.50381
- Lu, F., Dodson, J., Zhang, W., and Yan, H. (2019). Mid to Late Holocene Environmental Change and Human Impact: A View from Central China. *Quat. Sci. Rev.* 223, 105953. doi:10.1016/j.quascirev.2019.105953
- Ma, T., Zheng, Z., Rolett, B. V., Lin, G., Zhang, G., and Yue, Y. (2016a). New Evidence for Neolithic rice Cultivation and Holocene Environmental Change in the Fuzhou Basin, Southeast China. *Veget. Hist. Archaeobot.* 25, 375–386. doi:10.1007/s00334-016-0556-0
- Ma, T., Tarasov, P. E., Zheng, Z., Han, A., and Huang, K. (2016b). Pollen- and Charcoal-Based Evidence for Climatic and Human Impact on Vegetation in the Northern Edge of Wuyi Mountains, China, during the Last 8200 Years. *The Holocene* 26, 1616–1626. doi:10.1177/0959683616641744
- Marchitto, T. M., Muscheler, R., Ortiz, J. D., Carriquiry, J. D., and van Geen, A. (2010). Dynamical Response of the Tropical Pacific Ocean to Solar Forcing during the Early Holocene. *Science* 330, 1378–1381. doi:10.1126/science.1194887
- Mayewski, P. A., Rohling, E. E., Curt Stager, J., Karlén, W., Maasch, K. A., Meecker, L. D., et al. (2004). Holocene Climate Variability. *Quat. Res.* 62, 243–255. doi:10.1016/j.yqres.2004.07.001
- Nesbitt, H., and Markovics, G. (1997). Weathering of Granodioritic Crust, Long-Term Storage of Elements in Weathering Profiles, and Petrogenesis of Siliciclastic Sediments. *Geochim. Cosmochim. Acta* 61, 1653–1670.
- Nesbitt, H. W., Markovics, G., and Price, R. C. (1980). Chemical Processes Affecting Alkalis and Alkaline Earths during continental Weathering. *Geochimica et Cosmochimica Acta* 44, 1659–1666. doi:10.1016/0016-7037(80)90218-5
- Nesbitt, H. W., and Young, G. M. (1982). Early Proterozoic Climates and Plate Motions Inferred from Major Element Chemistry of Lutites. *Nature* 299, 715–717. doi:10.1038/299715a0
- Oppo, D. W., Mcmanus, J. F., and Cullen, J. L. (2003). Deepwater Variability in the Holocene Epoch. *Nature* 422, 277. doi:10.1038/422277b
- PAGES 2k Consortium (2013). Continental-scale Temperature Variability during the Past Two Millennia. *Nat. Geosci.* 6, 339–346. doi:10.1038/ngeo1797
- Pei, W., Wan, S., Clift, P. D., Dong, J., Liu, X., Lu, J., et al. (2020). Human Impact Overwhelms Long-Term Climate Control of Fire in the Yangtze River Basin since 3.0 Ka BP. *Quat. Sci. Rev.* 230, 106165. doi:10.1016/j.quascirev.2020.106165
- Peterson, L. C., and Haug, G. H. (2006). Variability in the Mean Latitude of the Atlantic Intertropical Convergence Zone as Recorded by Riverine Input of Sediments to the Cariaco Basin (Venezuela). *Palaeogeogr. Palaeoclimatol. Palaeoecol.* 234, 97–113. doi:10.1016/j.palaeo.2005.10.021
- Reimer, P. J., Austin, W., Bard, E., Bayliss, A., Blackwell, P., Ramsey, C., et al. (2020). The Intcal20 Northern Hemisphere Radiocarbon Age Calibration Curve (0–55 Cal kBP). *Radiocarbon* 100, 1–33.
- Revel, M., Ducassou, E., Grousset, F. E., Bernasconi, S. M., Migeon, S., Revillon, S., et al. (2010). 100,000 Years of African Monsoon Variability Recorded in Sediments of the Nile Margin. *Quat. Sci. Rev.* 29, 1342–1362. doi:10.1016/j.quascirev.2010.02.006
- Shah, R. A., Achyuthan, H., Lone, A. M., Kumar, S., Kumar, P., Sharma, R., et al. (2020). Holocene Palaeoenvironmental Records from the High-Altitude Wular Lake, Western Himalayas. *Holocene* 30, 733–743. doi:10.1177/0959683619895592journals.sagepub
- Shen, J., Wu, X., Zhang, Z., Gong, W., and Dong, H. (2013). Ti Content in Huguangyan Maar lake Sediment as a Proxy for Monsoon-Induced Vegetation Density in the Holocene. *Geophys. Res. Lett.* 40, 1–7. doi:10.1002/grl.50740
- Shuman, B. (2012). Patterns, Processes, and Impacts of Abrupt Climate Change in a Warm World: the Past 11,700 Years. *Wires Clim. Change* 3, 19–43. doi:10.1002/wcc.152
- Sinha, A., Kathayat, G., Weiss, H., Li, H., Cheng, H., Reuter, J., et al. (2019). Role of Climate in the Rise and Fall of the Neo-Assyrian Empire. *Sci. Adv.* 5, eaax6656. doi:10.1126/sciadv.aax6656
- Situ, S. (1987). *The Development Research of the Land on the History of Hainan Island [M]*. Haikou: Hainan People's Publishing House, 58. (in Chinese).
- Steinhilber, F., Beer, J., and Fröhlich, C. (2009). Total Solar Irradiance during the Holocene. *Geophys. Res. Lett.* 36, L19704. doi:10.1029/2009gl040142
- Strong, D., Flecker, R., Valdes, P. J., Wilkinson, I. P., Rees, J. G., Michaelides, K., et al. (2013). A New Regional, Mid-holocene Palaeoprecipitation Signal of the Asian Summer Monsoon. *Quat. Sci. Rev.* 78, 65–76. doi:10.1016/j.quascirev.2013.07.034
- Stuiver, M., Reimer, P. J., Bard, E., Beck, J. W., Burr, G. S., Hughen, K. A., et al. (1998). INTCAL98 Radiocarbon Age Calibration, 24,000–0 Cal BP. *Radiocarbon* 40, 1041–1083. doi:10.1017/s0033822200019123
- Su, Y., Chu, G., Liu, Q., Jiang, Z., Gao, X., and Habertzelt, T. (2015). A 1400 Year Environmental Magnetic Record from Varved Sediments of Lake Xiaolongwan (Northeast China) Reflecting Natural and Anthropogenic Soil Erosion. *Geochem. Geophys. Geosyst.* 16, 3053–3060. doi:10.1002/2015gc005880
- Tan, L., Li, Y., Wang, X., Cai, Y., Lin, F., Lin, F., et al. (2020). Holocene Monsoon Change and Abrupt Events on the Western Chinese Loess Plateau as Revealed by Accurately Dated Stalagmites. *Geophys. Res. Lett.* 46, e2020GL090273. doi:10.1029/2020GL090273
- Tian, C. J., Ouyang, T. P., Zhu, Z. Y., Qiu, Y., Peng, X. C., and Li, M. K. (2013). Spatial Distribution of Magnetic Susceptibility and its Provenance Implication of Surface Sediments in the Sea Areas Around the Hainan Island. *Trop. Geogr.* 33, 666–673. (in Chinese with English abstract).
- Wan, S., Toucanne, S., Clift, P. D., Zhao, D., Bayon, G., Yu, Z., et al. (2015). Human Impact Overwhelms Long-Term Climate Control of Weathering and Erosion in Southwest China. *Geology* 43, 439–442. doi:10.1130/g36570.1
- Wang, Y., Cheng, H., Edwards, R. L., He, Y., Kong, X., An, Z., et al. (2005). The Holocene Asian Monsoon: Links to Solar Changes and North Atlantic Climate. *Science* 308, 854–857. doi:10.1126/science.1106296
- Wang, Z., Maotian, L., Ruihu, Z., Chencheng, Z., Yan, L., Saito, Y., et al. (2010). Impacts of Human Activity on the Late-Holocene Development of the Subaqueous Yangtze delta, China, as Shown by Magnetic Properties and Sediment Accumulation Rates. *Holocene* 21, 393–407. doi:10.1177/0959683610378885
- Wanner, H., Solomina, O., Grosjean, M., Ritz, S. P., and Jetel, M. (2011). Structure and Origin of Holocene Cold Events. *Quat. Sci. Rev.* 30, 3109–3123. doi:10.1016/j.quascirev.2011.07.010
- Wei, G., Li, X. H., Liu, Y., Shao, L., and Liang, X. (2006). Geochemical Record of Chemical Weathering and Monsoon Climate Change since the Early Miocene in the South China Sea. *Paleoceanography* 21, PA4214. doi:10.1029/2006pa001300
- White, A. F., and Blum, A. E. (1995). Effects of Climate on Chemical Weathering in Watersheds. *Geochimica et Cosmochimica Acta* 59, 1729–1747. doi:10.1016/0016-7037(95)00078-e
- Wu, D., Zhou, A., Liu, J., Chen, X., Wei, H., Sun, H., et al. (2015). Changing Intensity of Human Activity over the Last 2,000 Years Recorded by the Magnetic Characteristics of Sediments from Xingyun Lake, Yunnan, China. *J. Paleolimnol.* 53, 47–60. doi:10.1007/s10933-014-9806-2
- Wu, L., Fu, P., Xu, L., Wei, Y., Zhou, X., Li, Y., et al. (2017). Changes in the Source of Sedimentary Organic Matter in the Marginal Sea Sediments of Eastern Hainan Island in Response to Human Activities during the Past 200 Years. *Quat. Int.* 440, 150–159. doi:10.1016/j.quaint.2016.07.007
- Wu, W., Zheng, H., Hou, M., and Ge, Q. (2018). The 5.5 Cal Ka BP Climate Event, Population Growth, Circumscription and the Emergence of the Earliest

- Complex Societies in China. *Sci. China Earth Sci.* 61, 134–148. doi:10.1007/s11430-017-9157-1
- Wu, X., Zhang, Z., Xu, X., and Shen, J. (2012). Asian Summer Monsoonal Variations during the Holocene Revealed by Huguangyan Maar lake Sediment Record. *Palaeogeogr. Palaeoclimatol. Palaeoecol.* 323–325, 13–21. doi:10.1016/j.palaeo.2012.01.020
- Xu, F., Hu, B., Dou, Y., Song, Z., Yuan, S., et al. (2017). Prehistoric Heavy Metal Pollution on the continental Shelf off Hainan Island, South China Sea: from Natural to Anthropogenic Impacts Around 4.0 Kyr BP. *The Holocene* 28, 455–463. doi:10.1177/0959683617729445
- Xu, H., Yeager, K. M., Lan, J., Liu, B., Sheng, E., and Zhou, X. (2015). Abrupt Holocene Indian Summer Monsoon Failures: A Primary Response to Solar Activity? *The Holocene* 25, 677–685. doi:10.1177/0959683614566252
- Yan, H. M., Tian, X., Xu, F. J., Hu, B. Q., Yang, Y. M., Feng, J. W., et al. (2016). Sediment Provenance of Offshore Mud Area of the Eastern Hainan Island in South China Sea since the Mid-holocene. *Haiyang Xuebao* 38, 97–106. (in Chinese with English abstract).
- Yang, B., Braeuning, A., Johnson, K. R., and Yafeng, S. (2002). General Characteristics of Temperature Variation in China during the Last Two Millennia. *Geophys. Res. Lett.* 29, 381–384. doi:10.1029/2001gl014485
- Yang, Z. H., Jia, J. J., Wang, X. K., and Gao, J. H. (2013). Characteristics and Variations of Water and Sediment Fluxes into the Sea of the Top three rivers of Hainan in Recent 50 Years. *Mar. Sci. Bull.* 1, 015. (in Chinese with English abstract).
- Zeng, Z. X., and Zeng, X. Z. (1989). *Physicogeography of the Hainan Island*. Beijing, China: Science Press. (in Chinese).
- Zhang, J., Wang, D. R., Jennerjahn, T., and Dsikowitzky, L. (2013). Land-sea Interactions at the East Coast of Hainan Island, South China Sea: a Synthesis. *Continental Shelf Res.* 57, 132–142. doi:10.1016/j.csr.2013.01.004
- Zhao, Y., Chen, F., Zhou, A., Yu, Z., and Zhang, K. (2010). Vegetation History, Climate Change and Human Activities over the Last 6200years on the Liupan Mountains in the Southwestern Loess Plateau in central China. *Palaeogeogr. Palaeoclimatol. Palaeoecol.* 293, 197–205. doi:10.1016/j.palaeo.2010.05.020
- Zong, Y., Yu, F., Huang, G., Lloyd, J. M., and Yim, W. W.-S. (2010). Sedimentary Evidence of Late Holocene Human Activity in the Pearl River delta, China. *Earth Surf. Process. Landforms* 35, 1095–1102. doi:10.1002/esp.1970

Conflict of Interest: The authors declare that the research was conducted in the absence of any commercial or financial relationships that could be construed as a potential conflict of interest.

Copyright © 2021 Huang, Kong, Chen, Hu, Wang and Lin. This is an open-access article distributed under the terms of the Creative Commons Attribution License (CC BY). The use, distribution or reproduction in other forums is permitted, provided the original author(s) and the copyright owner(s) are credited and that the original publication in this journal is cited, in accordance with accepted academic practice. No use, distribution or reproduction is permitted which does not comply with these terms.